International Journal of Applied Ceramic Technology 10(1):72-78 (2013)
DOI: 10.1111/j.1744-7402.2011.02748.x

Deposition of Silicon Carbide and Nitride Based Coatings by Atmospheric Plasma Spraying

Zoltán Károly[a,*], Cecília Bartha[a], Ilona Mohai[a], Csaba Balázsi[b], István E. Sajó[a], János Szépvölgyi[a, c]

[a] Institute of Materials and Environmental Chemistry, Chemical Research Center, Hungarian Academy of Sciences, Budapest, 1025 Hungary

[b] Research Institute for Technical Physics and Materials Science, Budapest, 1525 Hungary

[c] Research Institute of Chemical and Process Engineering, University of Pannónia, Veszprém, Hungary,

Abstract

In this work atmospheric plasma spraying of SiC and Si_3N_4 was investigated. Plasma spraying of these ceramics raises several problems since they would tend to decompose instead of melting at elevated temperatures during the process. To circumvent this problem the non-oxide ceramics were deposited as a composite powder mixed with non-oxide ceramic particles resulting in a ceramic/ceramic composite structure. Our findings were that using such a composite feedstock powder both oxidation and decomposition of the non-oxide particles could be avoided. A vitrified phase was also developed in the coating.

1. Introduction

Silicon carbide (SiC) and silicon nitride (Si_3N_4) are advanced engineering materials each having a number of attractive properties such as high strength, hardness, wear- and corrosion resistance

The authors kindly acknowledge the financial support of the National Office for Research and Technology (NKTH, Project No.: OMFB-00252/2007)

which properties are retained even at high temperature, excellent thermal shock resistance, high thermal conductivity [1-2]. These properties enable their use in many applications as structural materials for grinding, bearing balls, cutting tools, engine parts, turbine blades or for advanced heat engines. Due to the still high production cost of these ceramic materials there is also a great demand to take advantage of these outstanding properties as coatings on structural parts especially in high temperature applications to protect the bulk material against potential chemical attacks, corrosion, wear and heat.

The most extensively used techniques to create coatings even up to several millimetres thickness at a considerable deposition rate are thermal spraying methods. In these methods the precursor powders are melted during flying through the flame and the molten droplets propelled against the surface where they splash and spread. Any materials that can be melted in the flame are suitable to be deposited. Out of the spraying methods, plasma spraying with the extra high temperature it can provide (9 000-14 000 K [2]) is capable of melting even ceramics of high melting point. However, spraying of some ceramics including mainly non-oxide ceramics frequently presents problem as with rising temperature they decompose before reaching the melting point [3,4]. This is the case with SiC and Si_3N_4 materials, as well. One can circumvent this problem if a composite coating structure is created, in which discrete particles of non-oxide ceramics are embedded into a matrix. The material of the matrix is usually a metal such as aluminium or copper [5-8] or an intermetallic compound [9]. In these cases the ceramic particles act as a reinforcement to improve the mechanical properties of the coating matrix and they comprise only a smaller proportion in the precursor powder and consequently in the coating as well. Its value typically varied between 10 and 30 wt%. Yet, this smaller quantity is sufficient to improve strength, creep resistance at higher temperature. Preparation of feedstock powder usually involves simple

mixing of the powders of the different constituents.

Only very few attempts have been made yet for preparing composite coatings with ceramic matrix, in which some non-oxide particles are dispersed [10-11]. In these cases, it is a prerequisite that the ceramic matrix could be melted in the flame otherwise strong bond cannot be established between the coating and the substrate, considering the fact that bond is primarily based on a mechanical anchoring effect.

In the present work we investigated plasma spray technique to prepare composite coatings that comprises SiC and Si_3N_4 particles dispersed in a ceramic matrix. For SiC particles Al_2O_3-TiO_2 matrix was selected, while Si_3N_4 particles was dispersed in a Sialon matrix. Even though both alumina-titania and the sialon matrix have high melting point, they definitely could be melted in the plasma. In order to compare the effect of the preparation techniques of the feedstock powders on the developed structure we applied different procedure for that. SiC was only mechanically mixed thoroughly with the matrix material. In contrast, in case of Si_3N_4 containing coating an agglomeration procedure ensured that each particle of the feedstock powder consisted of composite material.

2. Experimental

Feedstock preparation

The feedstock powders for atmospheric plasma spraying of the SiC and Si_3N_4-containing powders were differently prepared.

The SiC containing powder feedstock was made by mixing fine powders of commercial SiC (F 1200, Washington Mills) with AT13 (Sulzer Metco, Al_2O_3 + TiO_2 13wt%) in a 15 to 85 weight ratio in a planetary mill. This mixture was agglomerated into spherical grains using ethanol solution of tetraethyl silicate. In this way the surface of the particles was coated by a gelled thin

film. The granulates were then dried at 120°C for 4 hours and heated at 400°C for additional half an hour to remove the organic content and to condensate a silica film on the grains in order to prevent from oxidation during spraying.

The Si_3N_4 containing feedstock powders were prepared in series of consecutive milling and sintering processes to gain ultimately spherical grains with particle size of around 50 μm. In the first step various ceramic materials including Al_2O_3 (12wt%, ALCOA A16), Y_2O_3 (4wt%, HC Starck) and AlN (15wt%, HC Starck) were added to Si_3N_4 (69wt%) and mixed for 3 hours in a ball mill in ethanol. The mixed powder was then sintered for 30 minutes at 1730°C under 10 atm of nitrogen. In this way the ceramic mixture was in part transformed to Sialon. The as-prepared Sialon was ball milled further for additional 4 hours with the addition of Al_2O_3, Y_2O_3 and AlN to finally obtain the feedstock powder denoted Powder A. Another feedstock powder, denoted Powder B was also prepared by further mixing of powder A (75wt%) with Si_3N_4 (10wt%) and Al_2O_3 (15wt%). In this way, two batches of powders with similar morphology but slightly different crystalline phases were prepared. The main difference between powder A and B was that in powder A the Si_3N_4 content was converted entirely into Sialon during sintering, while powder B contained α-Si_3N_4 in 10wt%. The as-prepared feedstock materials comprised of grains with a broader size distribution. Considering that a narrow particle size is a prerequisite to achieve pore free coating only a sieved fraction of 50-125 μm grains were used for spraying.

Plasma spraying

The atmospheric plasma spraying was carried out with a commercial plasma spray gun (Metco 9MB). The main operating conditions including the applied voltage, current, gas flow rates and powder feed rate are summarized in Table 1. The substrates to be coated were heat resistant steel sheets (AISI 310), which were grit blasted by corundum prior to spraying to enhance adhesion of

the coating. The sheets were previously coated with a metallic "bond" layer of 50 μm thickness to create a transition layer in terms of heat expansion. The bond powder composed of NiCoCrAlY alloy with particle size of 60 μm. In all cases, right before plasma spraying the metal sheet was preheated up to 250-300°C.

Characterization

Particle size distribution of starting powders was analyzed by laser diffraction method using a Malvern Mastersizer 2000 device. Morphology of the feedstock materials and structure of the coatings was characterized by SEM Philips XL30 model. The feedstock powders and the coating were characterized by X-ray diffraction using CuKα radiation (typically 40 kV, 40mA) to determine the phases.

3. Results and discussion

Morphology of feedstock powder

Fig. 1 shows the SEM image of the feedstock powder after agglomeration. Even though the grains are composed of agglomerated fine particulates of various components, they were easy to feed owing to the nearly spherical, free falling grains. The particle size of the prepared powders was somewhat broader according to LDA analysis (Fig. 2). Since the APS process can be optimized only to a narrow particle size range, the size distribution of the feedstock powder profoundly affects the developing microstructure of the coating. Grains larger than the optimal (assuming the mean size) tend to incorporate into the coating without melting and thus gives rise to a porous structure. To avoid this problem preliminary sieving was applied. Nevertheless, the SiC and Si_3N_4 particles mixed in the grains are unable to melt anyway. Due to their small size as compared to the size of the feedstock grains and their relatively lower ratio in the grains,

however, they may be completely embedded into the molten matrix.

Fig. 1, Fig. 2

Using XRD analysis we could check whether or not any phase changes or vitrification occurred during feedstock preparation. The different constituents of the SiC-containing feedstock powder i.e. SiC, Al_2O_3 and TiO_2 can be clearly identified on the X-ray diffractogram (Fig. 3).

On preparing the Si_3N_4-containing feedstock powders new phases were aimed to develop during sintering. According to XRD analysis (Fig. 4) the grains are composed of different crystalline phases including β-Sialon, corundum and yttrium aluminate garnet (YAG) without any glassy phase. The main difference between powder A and B is that the latter contains additional crystalline phases such as α-Si_3N_4 and Y_2O_3, as well.

Fig. 3, Fig. 4

3.1 SiC – alumina – titania composite coating

SEM images of the cross section of the coated steel sheet (Fig. 5) show a quite even ceramic layer with a thickness of 200 μm. At larger magnification, however, considerable amount of pores become visible in the coating. In typical cases the particles are melted in the plasma flame during flight and the substrate is coated by non-porous droplets. Porosity, if occurs is assumed to be created as a result of gaps between splats or splat curl up [12]. However, when the grains are composed of non-melting carbide particles another aspect must be considered. The initial porosity of the grains may not completely disappear before impact by the wetting effect of the surrounding molten phase. This can also contribute to the overall porosity of the coating especially in the case of bigger grains. This also applies to grains that could not melt at all because of their unfavorable thermal history.

Figs. 5

On atmospheric plasma spraying of SiC containing powder mixture we face two risks. One is the oxidation of SiC particles on getting into contact with ambient air at elevated temperature, while the other one is the possible decomposition of SiC before being able to melt at the high temperature of the plasma flame [13]. In addition, interactions of SiC and Al_2O_3 and TiO_2 may also occur that results in the decomposition of SiC [14]. On the other hand, the injected powder has to be subjected to high temperature, at least above 2050°C, at which the alumina-titania mixture, the matrix forming components of the composite ceramic coating melts [15]. Considering that only characteristic peaks of Al_2O_3 and SiC can be identified on the X-ray diffractogram of the coating (Fig. 3), one can conclude that both decomposition and considerable oxidation of SiC could be prevented. However, the rapid cooling of the molten droplets had twofold effects on the phase structure of the coating. On the one hand, it gave rise to the formation of a vitrified phase. On the other hand, considerable part of the α-alumina present in the feedstock powder was re-crystallized as γ-phase in the coating. It has been experienced earlier [16-17] that molten alumina droplets crystallize in thermodynamically less stable phases on rapid cooling instead of the α-phase. As a consequence, peaks of the α-phase is thus an indication that larger particles did not melt entirely during spraying and the unmelted α-phase in these particles acted as seeds for crystallization [10].

3.2 Si_3N_4-based composite coatings

The thickness of the coatings sprayed in different tests varied from a few hundred micrometers up to 2 mm. Porosity of the obtained ceramic layer becomes apparent on the SEM image of the coating (Fig. 6) comparing with the metallic bond layer underneath. This porosity again can be attributed to the non-melting Si_3N_4 particles in the grains. In addition the size distribution of

feedstock powder was also wide, which may cause the incorporation of several larger non-melted agglomerates into the coating.

Fig. 6

X-ray diffractograms suggest (Fig. 7) formation of a glassy phase in the coatings. The peaks correspond to the crystalline phases of β-Sialon, corundum, yttrium-oxide and yttrium aluminium oxide, as well. In addition, α-Si_3N_4 could also be detected in the coating prepared from powder B, which means that its oxidation during spraying could be prevented by the powder preparation technique. Although Si_3N_4 is considered to be oxidation resistant material, above 1200°C it also starts to oxidize [18]. However, being mixed inside grains and surrounded by molten Sialon during spraying, it could be preserved from oxidation. The distribution of the corresponding crystalline phases is summarized in Table 2. Comparing the phase composition of the starting material with that of particular coatings in Table 2 it can be concluded that most of the YAG phase in Powder A was vitrified due to rapid cooling. Glassification of YAG phase on plasma spraying was also observed by others [19-21]. Although, YAG theoretically could also be decomposed to Al_2O_3 and $YAlO_3$ the absence of the latter on the XRD plot suggests that this decomposition did not occurred. The apparent increase of β-Sialon and α-Al_2O_3 phases can be thus attributed to the relative decrease of the crystalline phases. In coating B both α-Al_2O_3 and Y_2O_3 decreased comparing with Powder B, while YAG phase appeared. It suggests that during spraying YAG formation took place between the two mentioned phases. In contrast to Coating A, however, glass phase did not formed.

Fig. 7

4. Conclusions

Even though atmospheric plasma spraying is a well known and commonly used technique to prepare thick metal or ceramic coatings on various substrates, spraying of certain ceramic materials which tend to decompose at higher temperature before melting still involves difficulties. In this work plasma spraying of SiC and Si_3N_4 containing ceramic composite powders were investigated. The coating preparation consisted of two major steps: preparation of the composite agglomerated grains suitable to spraying and plasma spraying under the optimal conditions. Preparation of feedstock powders from a few micrometer-sized particles by consecutive attrition and sintering resulted in a wide particle size distribution ranging from 30-200 μm that was sieved before spaying below 125 μm. This powder then could be easily fed into the plasma flame. The resulted few hundred micrometer thick coatings have considerable porosity. Although part of the ceramic constituents were vitrified on spraying the SiC and Si_3N_4 particles could be prevented both from oxidation and decomposition and were embedded into the matrix without any phase change.

Acknowledgment

The authors kindly acknowledge the financial support of the National Office for Research and Technology (NKTH, Project No.: OMFB-00252/2007)

References

[1] W. E. Lee, W. M. Rainforth, *Ceramic Microstructures*, Chapman & Hall, 415-418, London, 1985.

[2] P. Fauchais, G. Montavon, M. Vardelle, J. Cedelle, “Developments in direct current plasma spraying,” *Surf Coat Tech.,* 201 1908–1921 (2006).

[3] K.A. Schwetz, R. Riedel (Ed.), *Handbook of Ceramic Hard Materials*, vol. 1, Wiley-VCH, 683–740, Weinheim, 2000.

[4] Hyun-Ki Kang, Suk Bong Kang, "Thermal decomposition of silicon carbide in a plasma-sprayed Cu/SiC composite deposit," *Mat. Sci & Eng. A,* 428 [1-2] 336-345 (2006).

[5] B. Torres, M. Campo, J. Rams, "Properties and microstructure of Al–11Si/SiCp composite coatings fabricated by thermal spray," *Surf. Coat. Tech.,* 203 1947-1955 (2009).

[6] J. Rams, M. Campo, B. Torres, A. Urena, "Al/SiC composite coatings of steels by thermal spraying," *Materials Letters,* 62 2114-2117 (2008).

[7] M. Campo, M.D. Escalera, B. Torres, J. Rams, A. Urena, "Wear behaviour of coatings of aluminium matrix composites fabricated by thermal spray method," *Revista de Metallurgia,* 43[5] 359-369 (2007).

[8] Hyun-Ki Kang, Suk Bong Kang, „Thermal decomposition of silicon carbide in a plasma-sprayed Cu/SiC composite deposit," *Mat. Sci. & Eng. A,* 428 336-345 (2006)

[8] S.M. Hashemi, M.H.Enayati, M.H. Fathi, "Plasma Spray Coatings of Ni-Al-SiC Composite," *J. Thermal Spray Techn.,* 18 [2] 284-291 (2009).

[10] M. U. Devi, "On the nature of phases in Al2O3 and Al2O3–SiC thermal spray coatings," *Ceram. Int.* 30 [4] 545-553 (2004).

[11] S. Thiele, R.B. Heimann, M. Herrmann, M. Nebelung, T. Schnick, B. Wielage, P. Vuoristo, "Microstructure and Properties of Thermally Sprayed Silicon Nitride-Based Coatings," *J. Thermal Spray Tech.*, 11 [2] 218-225 (2002).

[12] R. Ghafouri-Azar, J. Mostaghimi, S. Chandra, "A stochastic model of plasma sprayed coating formation," Proceedings of the 15th International Symposium on Plasma Chemistry, Orléans, France, July 9-13, 2001.

[13] W. Wesch, “Silicon carbide: Synthesis and Processing”, *Nucl. Instrum. Meth. B* 116 305-321 (1996).

[14] J. Ihle, M. Herrmann, J. Adler, “Phase formation in porous liquid phase sintered silicon carbide: Part I: Interaction between Al_2O_3 and SiC”, *J. Eur. Ceram. Soc.* 25 987–995 (2005).

[15] L. Li, Z. J. Tang, W. Y. Sun, and P. L. Wang, “Phase diagram prediction of the Al_2O_3-SiO_2-La_2O_3 system” *J. Mater. Sci. Technol.*, (Shenyang, People's Repub. China), 15 439-443 (1999).

[16] Z. Károly, J. Szépvölgyi, “Plasma Spheroidization of Ceramic Particles,” *Chem. Eng. and Proc.,* 44 221-224 (2005).

[17] Z. Yin, S. Tao, X. Zhou, C. Ding, “Microstructure and mechanical properties of Al2O3–Al composite coatings deposited by plasma spraying,” *Appl. Surf. Sci.*, 254 1636-1643 (2008).

[18] V. A. Lavrenko, P. P. Pikuza, E. S. Lugovskaya, V. V. Shvaiko, “High-temperature oxidation of silicon nitride powders” *Powder Met. and Metal Ceram.* 24 5 390-393 (1985).

[19] I. Lin, A. Navrotsky, J.K. Richard Weber, P.C. Nordine, “Thermodynamics of glass formation and metastable solidification of molten $Y_3Al_5O_{12}$” *J. Non-Cryst. Solids* 243 273-276 (1999).

[20] Ravi BG, A.S. Gandhi, X.Z. Guo, J. Margolies, S. Sampath, “Liquid precursor plasma spraying of functional materials: A case study for yttrium aluminum garnet (YAG)”, *J. Thermal Spray Tech.* 17 [1] 82-90 (2008).

[21] M. Suzuki, S. Sodeoka, T. Inoue, “Control of structure and properties on Al2O3/YAG composite coating prepared by plasma spray process” *J. Jpn I. Met.* 69 1 23-30 (2005).

Figure captions

Fig. 1 SEM image of the Si_3N_4 composite feedstock powder after sieving

Fig. 2 Particle size distribution of feedstock powders; SiC denotes SiC-containing powder, while Powder A and B denotes Si_3N_4-containing powders

Fig. 3 X-ray diffractogram of the SiC-alumina-titania feedstock powder and composite coating

Fig. 4 X-ray diffractogram of the Si_3N_4 based feedstock powders

Fig. 5 SEM image of the cross section of SiC composite coating

Fig. 6 SEM image of the cross section of Si_3N_4 composite coating (The ca. 200 μm thick brighter area from the right is attributed to the upper surface of the specimen)

Fig. 7 X-ray diffractogram of the Si_3N_4 based composite coating

Table 1. Plasma spraying parameters for bond powder and composite powders

Parameters	Bond powder	Composite powders
Voltage (V)	80	100
Current (A)	450	490
Plate power (kW)	36	49
Primary gas flow rate (slpm*)	Ar – 42	Ar – 38
Secondary gas flow rate (slpm)	H_2 – 5	H_2 – 13
Carrier gas flow rate (slpm)	Ar – 10	Ar – 7
Powder feed rate ($g \cdot min^{-1}$)	50	14
Spray distance (mm)	100	120

* standard liter per minute

Table 2. The crystalline phases detected in the feedstock powders and the corresponding coatings and their approximate distribution

	β-Sialon	α-Al_2O_3	α-Si_3N_4	Y_2O_3	YAG
Powder A	20	20	-	-	40
Powder B	30	35	10	15	-
Coating A	30	30	-	3	10
Coating B	35	30	10	5	20

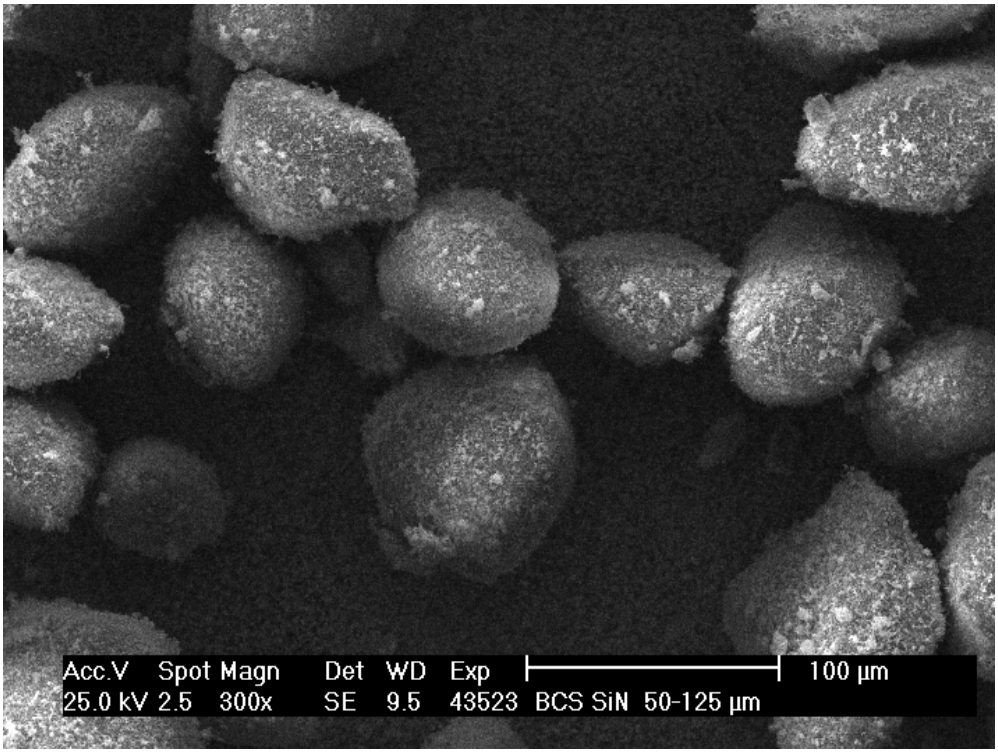
Acc.V Spot Magn Det WD Exp 100 µm
25.0 kV 2.5 300x SE 9.5 43523 BCS SiN 50-125 µm

Fig.1

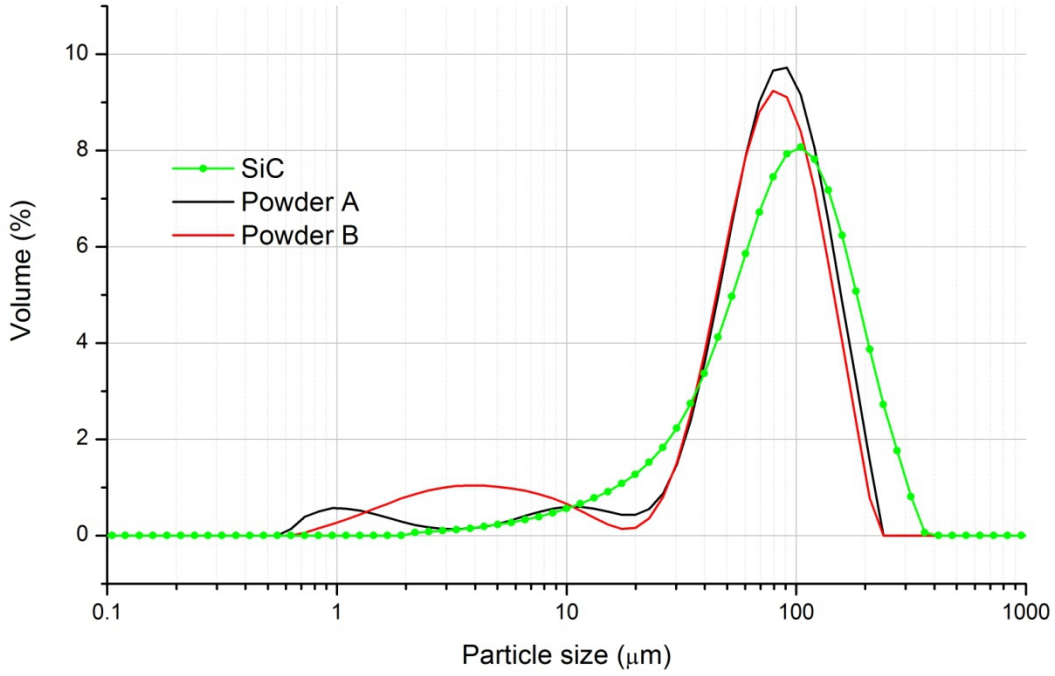
SiC
Powder A
Powder B
Volume (%)
Particle size (μm)
0
2
4
6
8
10
0.1
1
10
100
1000

Fig.2

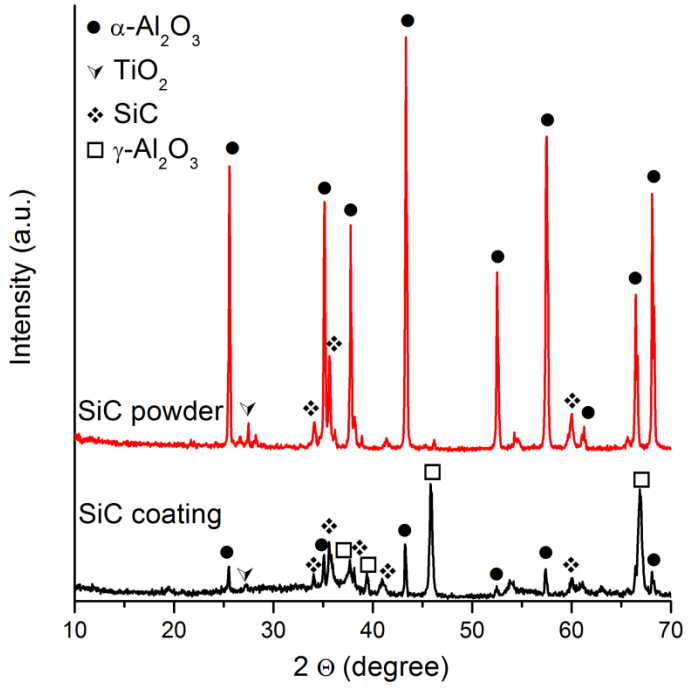
α-Al2O3
TiO2
SiC
γ-Al2O3
SiC powder
SiC coating
Intensity (a.u.)
2 Θ (degree)
10
20
30
40
50
60
70

Fig.3

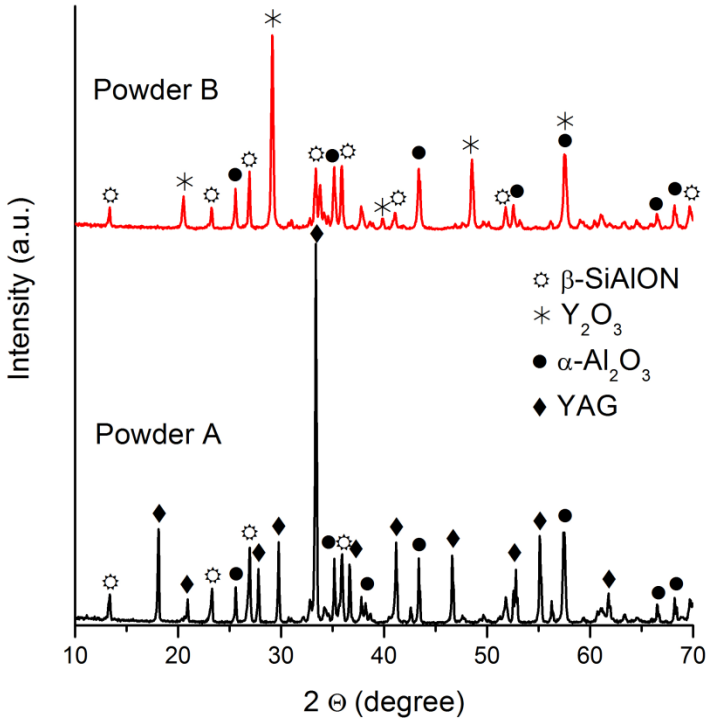
Powder B
Powder A
Intensity (a.u.)
β-SiAlON
Y2O3
α-Al2O3
YAG
10
20
30
40
50
60
70
2 Θ (degree)

Fig.4

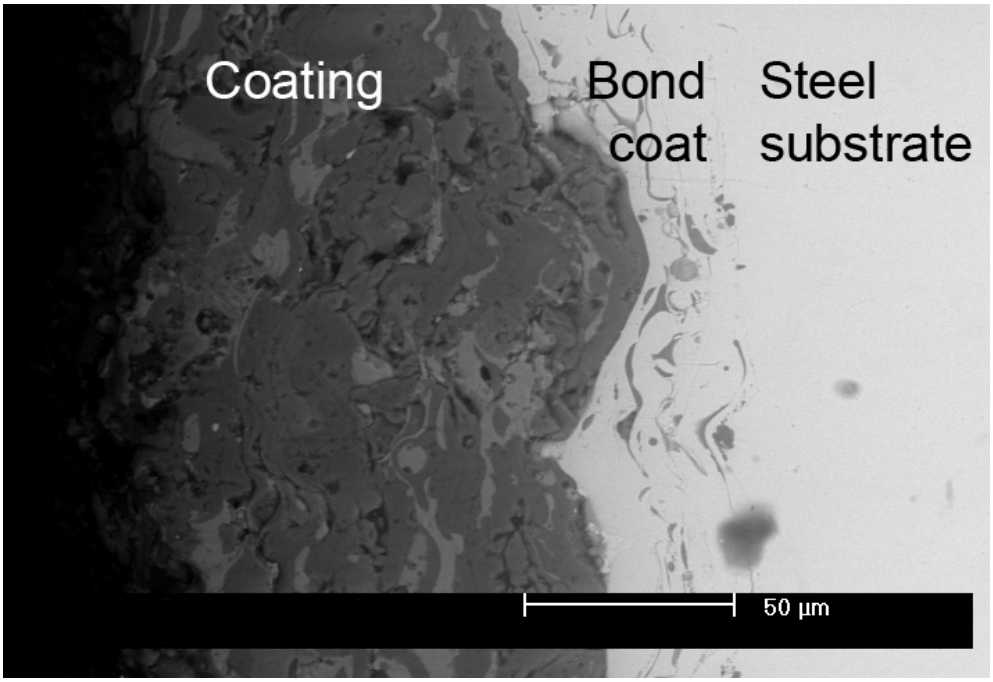
Coating
Bond coat
Steel substrate
50 µm

Fig.5

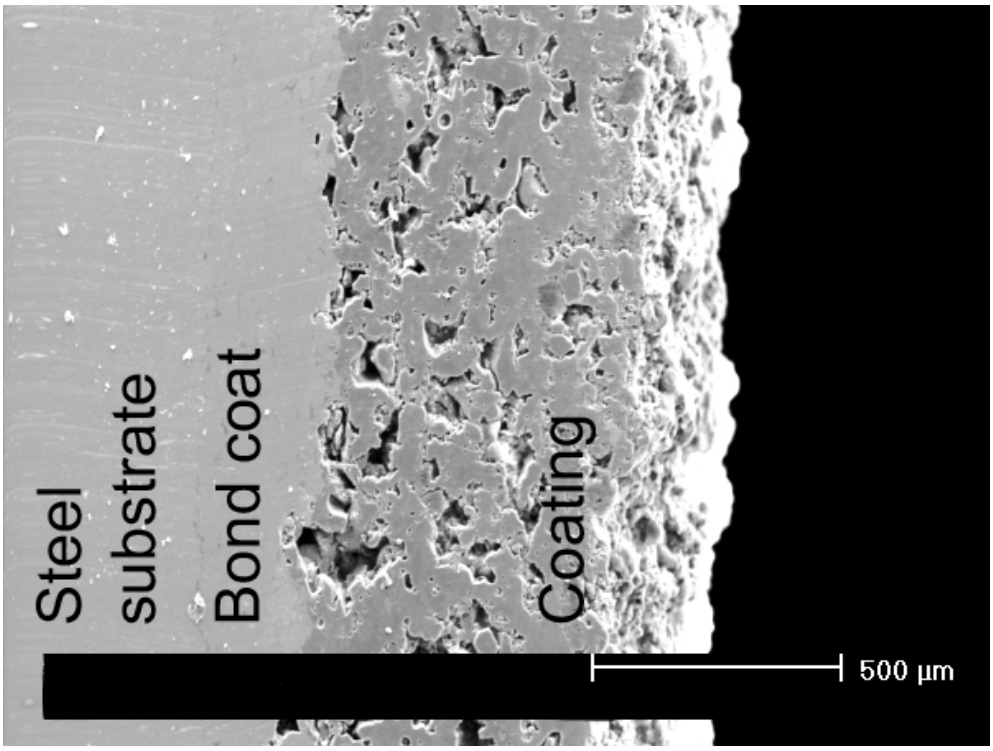

Fig.6

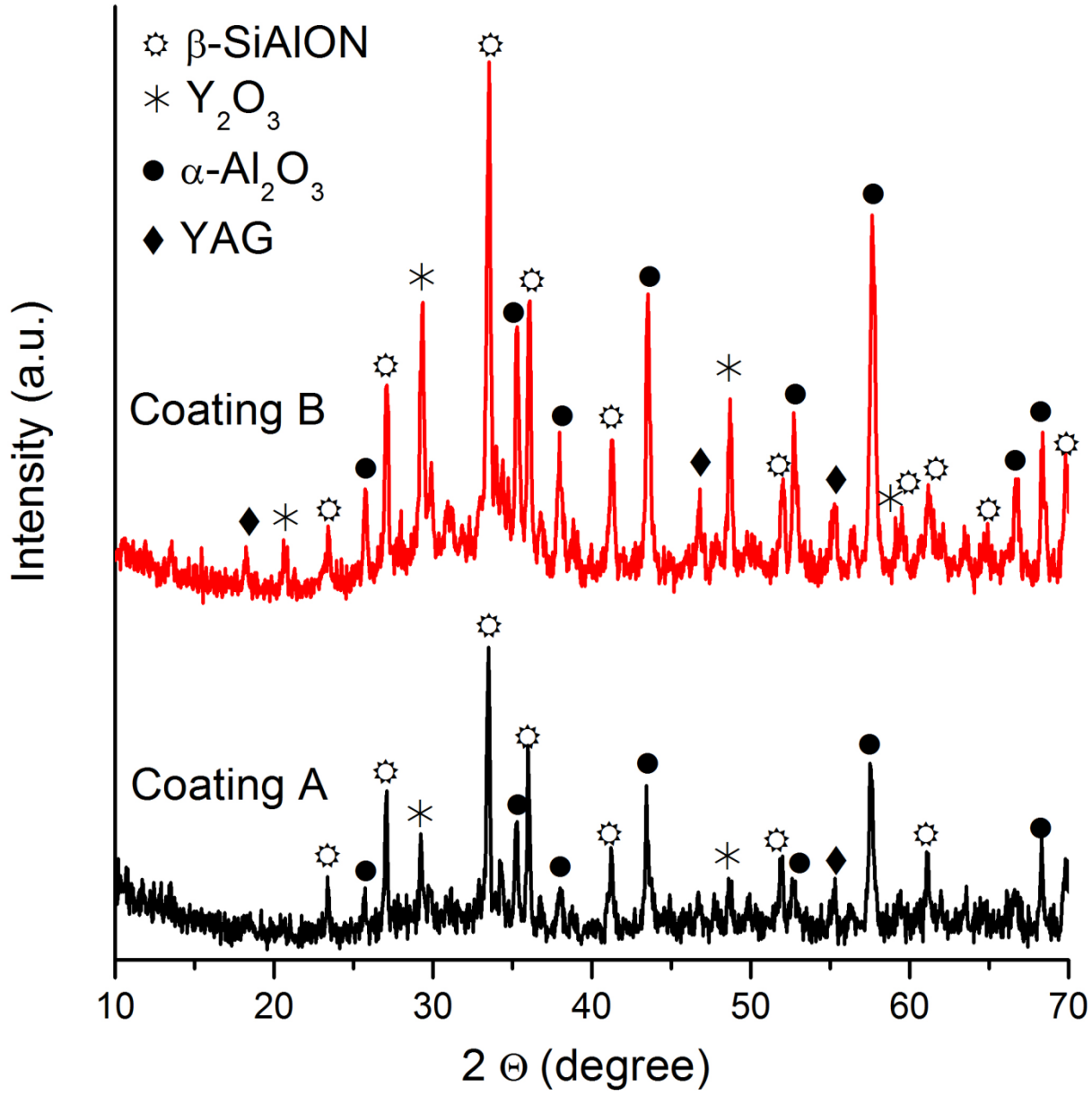
β-SiAlON
Y2O3
α-Al2O3
YAG
Coating B
Coating A
Intensity (a.u.)
10
20
30
40
50
60
70
2 Θ (degree)

Fig.7